

Supporting Information to the paper

Green one-pot synthesis and processing of polyimide-silica hybrid materials

by

Lukas Leimhofer^a, Bettina Baumgartner^a, Michael Puchberger,^a Thomas Prochaska^b,
Thomas Konegger^b and Miriam M. Unterlass^{a*}

^aTechnische Universität Wien, Institute of Materials Chemistry, , Getreidemarkt 9/BC/2, A-1060 Vienna, Austria.

^bTechnische Universität Wien, Institute of Technology and Analytics, Getreidemarkt 9/BB/2, A-1060 Vienna, Austria

*corresponding author: *miriam.unterlass@tuwien.ac.at*

1. Experimental section	2
1.1 Used Chemicals	2
1.2 Polymer synthesis	2
1.3 Compaction molding	4
2. Characterization of and PI6 and PI6/SiO₂-hybrids	4
2.1 FT-IR-ATR analysis	4
2.2 Powder X-ray diffraction (pXRD)	9
2.3 Scanning electron microscopy (SEM)	11
2.4 Energy-dispersive X-ray spectroscopy (EDAX)	14
2.5 Cross Polarization Magic Angle Spinning Nuclear Magnetic Resonance Spectroscopy (CP-MAS-NMR)	18

1. Experimental section

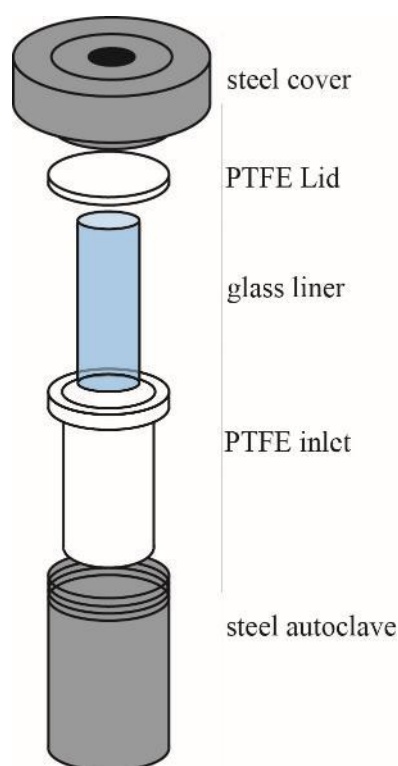
1.1 Used Chemicals

Hexamethylene diamine (HMDA, Sigma Aldrich) used as received; pyromellitic acid (PMA Sigma Aldrich) used as received; tetraethoxysilane (TEOS, Sigma Aldrich) used as received; (3-aminopropyl)triethoxysilane (APTES, Sigma Aldrich) used as received;

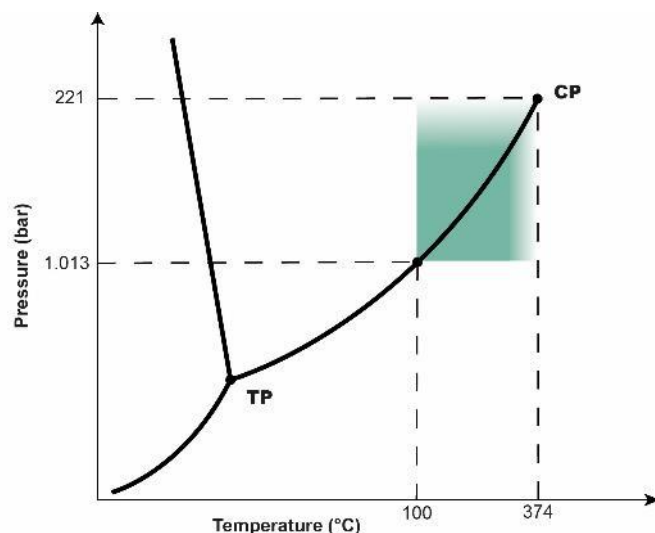
1.2 Polymer synthesis

Hydrothermal pathway (small scale):

A dispersion of both monomers (HMDA and PMA) in 15 mL deionised water and was prepared in a cylindric glass liner ($V = 27$ mL). For the synthesis of the PI-hybrid materials the silicon alkoxides, tetraethoxy orthosilane (TEOS) and/or aminopropyltriethoxysilane (APTES) were additionally added while stirring. The liner was then transferred into a non-stirred autoclave ($V = 45$ mL), equipped with a Teflon liner (see scheme 1). The autoclave was then placed into a preheated oven at different temperatures (140 °C or 200 °C) and kept there for various reaction times ($2 - 72$ h). At the end of the reaction, the autoclave was quickly cooled back to room temperature in tap water. HT-PI and HT-PI6/SiO₂-hybrid phases were isolated, washed 3 times with approximately 20 mL distilled water and dried *in vacuo* at RT in a dessicator for at least 24 h.



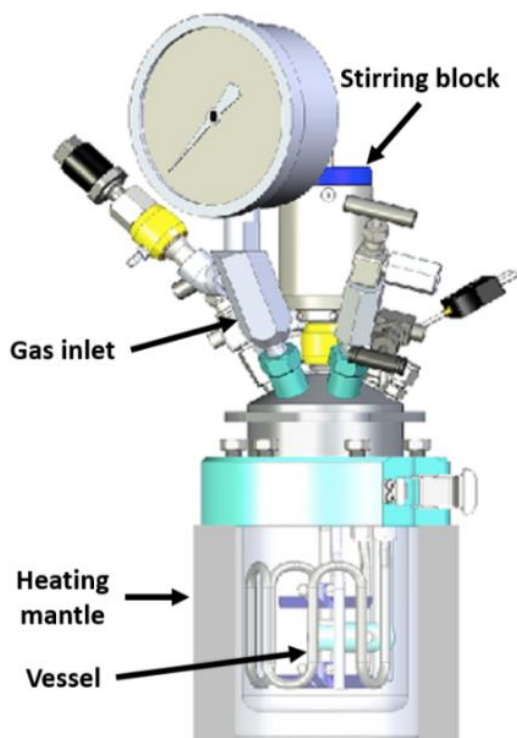
Scheme 1: Schematic of used steel autoclave



Scheme 2: Phase diagram of H₂O: green area illustrates the hydrothermal regime above 100°C and below the critical point; TP=triple point and CP=critical point

Hydrothermal pathway (upscaling)

A dispersion of hexamethyldiamine (HDMA) and pyromellitic acid (PMA) was prepared with 400mL of deionised water in a glass liner (V=1000 mL). For the synthesis of the PI6/SiO₂ hybrid material, the calculated amount of tetraethoxysilane (TEOS) and (3-aminopropyl)triethoxysilane (APTES) were additionally added. The liner was then transferred to a batch autoclave and heated up to 200 °C stirring constantly. The temperature was held for 24 h before cooling back to RT with cold tap water. The obtained white powder was filtered, carefully washed with deionised water and dried at RT under reduced pressure in a desiccator for at least 24 h.



Scheme 3: Schematic of used batch autoclave

1.3 Sintering process - compaction molding

In this work, the particulate starting products were filled into a steel cavity (diameter: 40 mm) and compacted uniaxially at a pressure of 80 MPa (P.O. Weber laboratory press). Kapton foil was used to avoid fusing of the specimen to the top and bottom punches. After compaction, the die was heated to 300 °C and held at this temperature for 2 h. If required, the compaction pressure was readjusted accordingly. After cooling to 50 °C, the pressure was released and the cylindrical specimen was ejected from the mold.

2. Characterization of and PI6 and PI6/SiO₂-hybrids

2.1 FT-IR-ATR analysis

FT-IR-ATR spectra were recorded on a Bruker Tensor 27 working in ATR MicroFocusing MVP-QL with a diamond crystal, using OPUS (version 4.0) software for data analysis. Resolution was set to 2-4 cm⁻¹, and spectra were recorded from 4000 to 600 cm⁻¹.

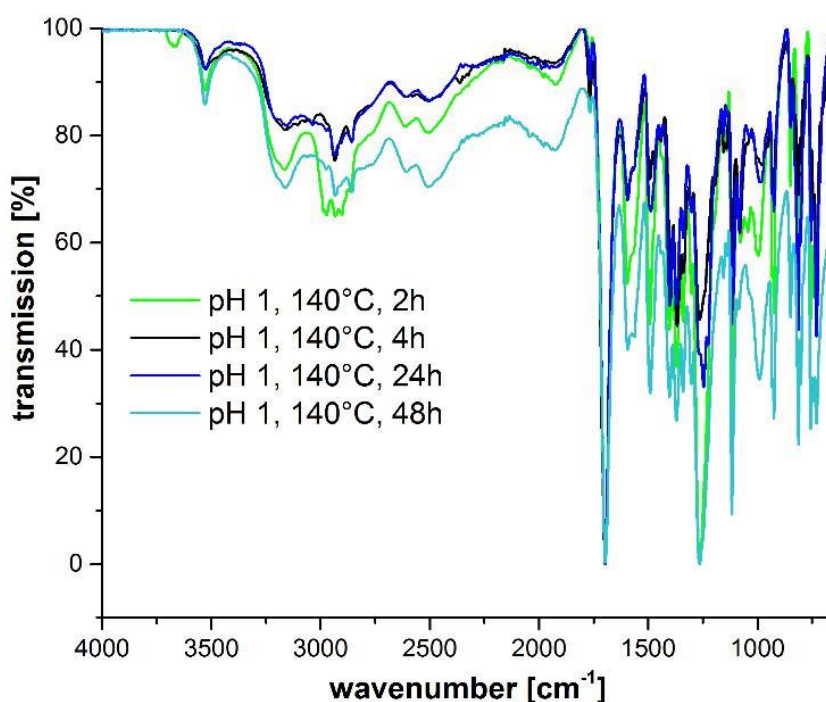


Figure 1: shows a superimposition of normalized FT-IR-ATR spectra of PIs synthesized at 140°C and pH 1 after different reaction times. Even after 48 h the PI contains monomer salt and crystal water indicated by a high number of broad modes (3750-2250 cm⁻¹)

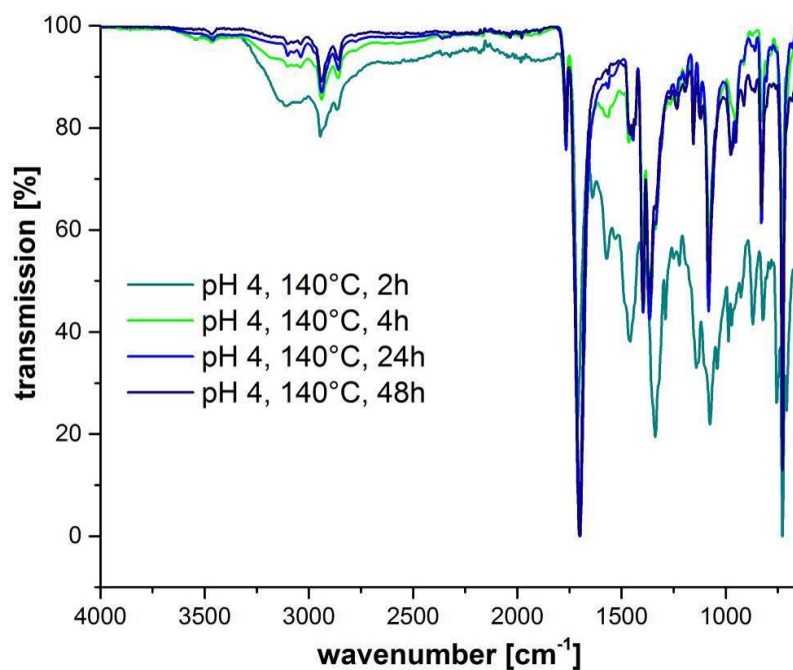


Figure 2: Superimposition of normalized FT-IR-ATR spectra of PIs synthesized at 140 °C and pH 4 after different reaction times , PI6 after 48 h appears nearly complete. ($\tilde{\nu}_{s,C=O}(\approx 1765 \text{ cm}^{-1})$, $\tilde{\nu}_{as,C=O} \approx 1700 \text{ cm}^{-1}$)

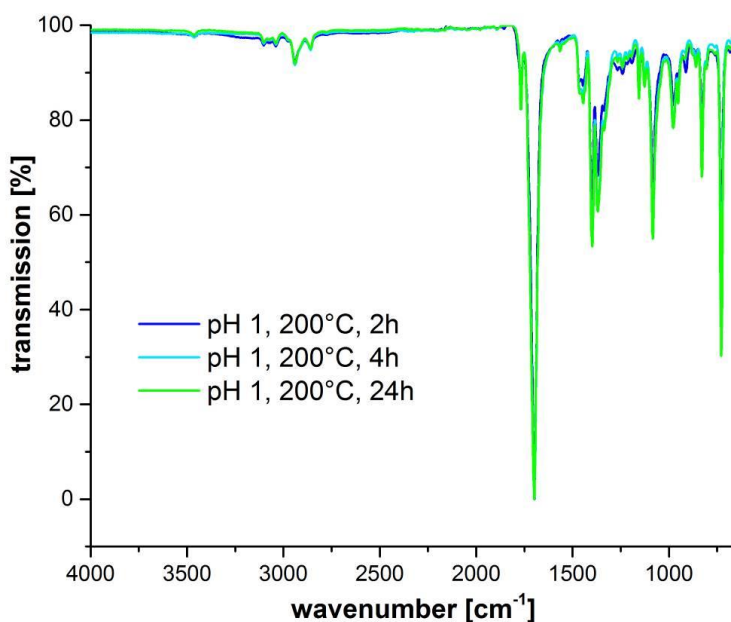


Figure 3: Superimposition of normalized FT-IR-ATR spectra of PIs synthesized at 200 °C and pH 1 after different reaction times. Full conversion after $t_R = 2 \text{ h}$: ($\tilde{\nu}_{s,C=O}(\approx 1765 \text{ cm}^{-1})$, $\tilde{\nu}_{as,C=O} \approx 1700 \text{ cm}^{-1}$ and $\tilde{\nu}_{ar-H}$: 3101 and 3035 cm^{-1} ; $\tilde{\nu}_{alkyl-H}$: 2941, 2858 cm^{-1})

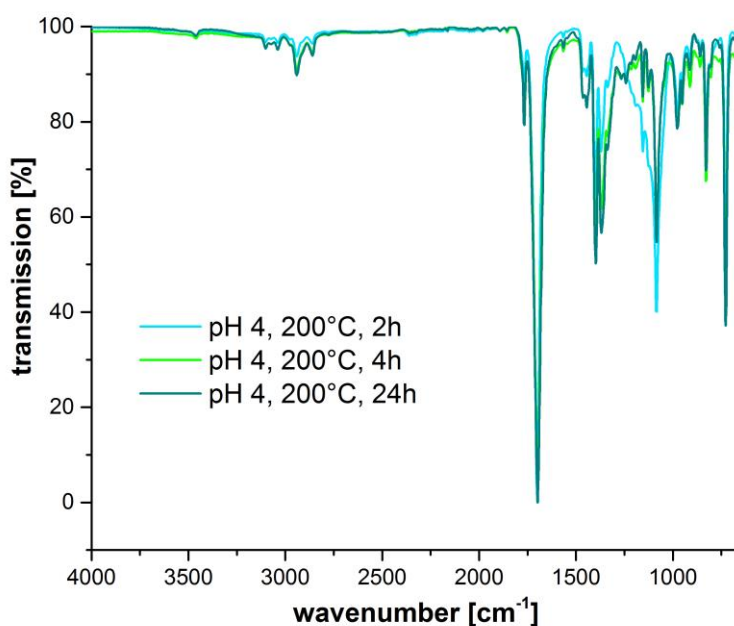


Figure 4: Superimposition of normalized FT-IR-ATR spectra of PIs synthesized at 200°C and pH 4 after different reaction times. Full conversion after $t_R = 2h$: ($\tilde{\nu}_{s,C=0} \approx 1765 \text{ cm}^{-1}$, $\tilde{\nu}_{as,C=0} \approx 1700 \text{ cm}^{-1}$ and $\tilde{\nu}_{ar-H}$: 3101 and 3035 cm^{-1} ; $\tilde{\nu}_{alkyl-H}$: 2941, 2858 cm^{-1})

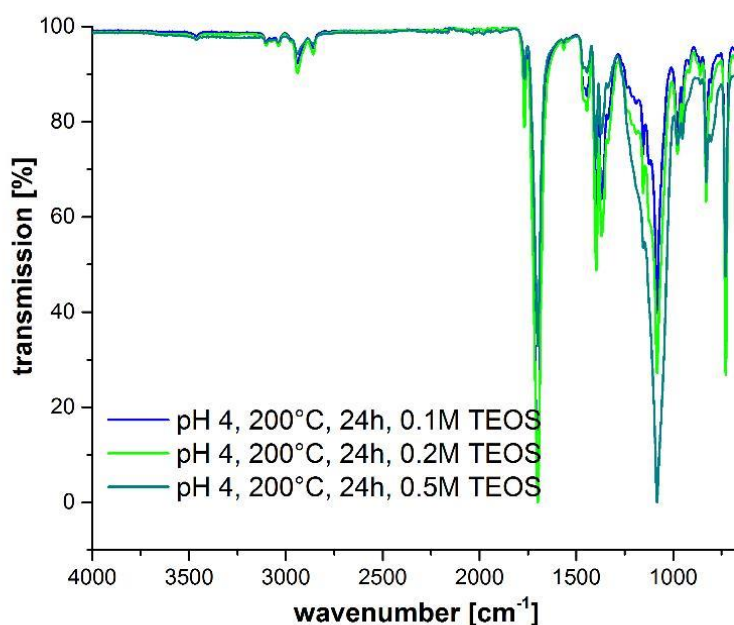


Figure 5: Superimposition of normalized FT-IR-ATR spectra of PI-SiO₂-hybrids synthesized at 200 °C and pH 4 with different TEOS concentrations. Full conversion after all t_{RS} ($\tilde{\nu}_{s,C=0} (\approx 1765 \text{ cm}^{-1})$, $\tilde{\nu}_{as,C=0} \approx 1700 \text{ cm}^{-1}$ and $\tilde{\nu}_{ar-H}$: 3101 and 3035 cm^{-1} ; $\tilde{\nu}_{alkyl-H}$: 2941, 2858 cm^{-1}). Siloxane vibration is also present ($\tilde{\nu}_{as} (\text{Si-O-Si}) \approx 1080 \text{ cm}^{-1}$) and grows with increasing TEOS amount.

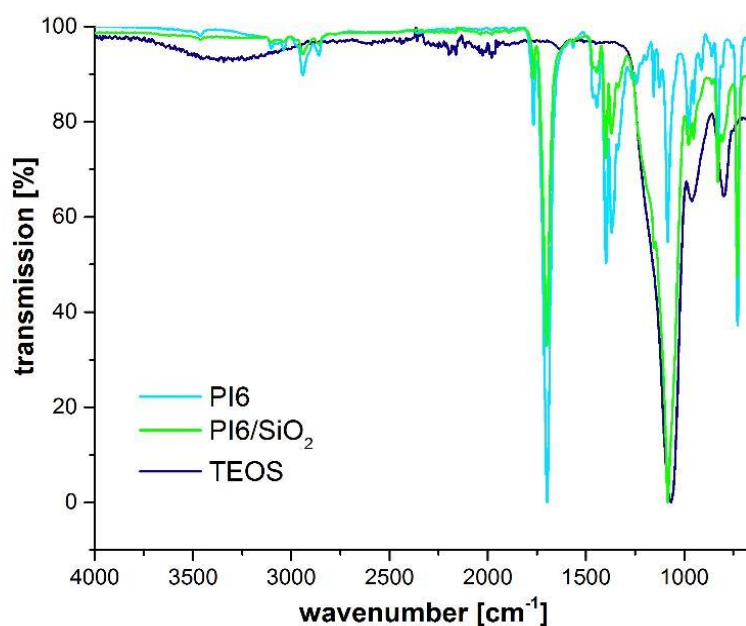


Figure 6: Shows a superimposition of normalized FT-IR-ATR spectra of PI6/SiO₂-hybrid, PI6 and silica (labelled as TEOS in figure) synthesized at 200°C and pH 4 after 24h. SiO₂ prepared hydrothermally shows characteristic modes at $\approx 1080\text{ cm}^{-1}$ ($\tilde{\nu}_{as}$ (Si-O-Si)), ≈ 3250 and 960 cm^{-1} (Si-OH stretching and bending) and $\approx 800\text{ cm}^{-1}$ (Si-O bond bending).

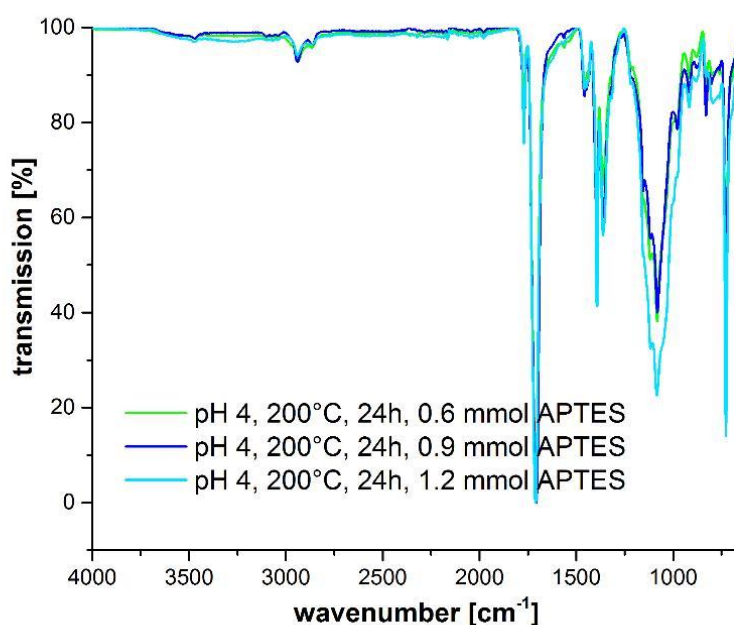


Figure 7: Superimposition of normalized FT-IR-ATR spectra of PI6/SiO₂-hybrids obtained from HDMA, PMA, APTES and TEOS (#4-6) at 200 °C and pH 4 with different APTES concentrations. Full conversion at all APTES concentrations ($\tilde{\nu}_{s,C=0} \approx 1765\text{ cm}^{-1}$, $\tilde{\nu}_{as,C=0} \approx 1700\text{ cm}^{-1}$ and $\tilde{\nu}_{ar-H}: 3101$ and 3035 cm^{-1} ; $\tilde{\nu}_{alkyl-H}: 2941, 2858\text{ cm}^{-1}$). Siloxane vibration is also present ($\tilde{\nu}_{as}$ (Si-O-Si) $\approx 1080\text{ cm}^{-1}$)

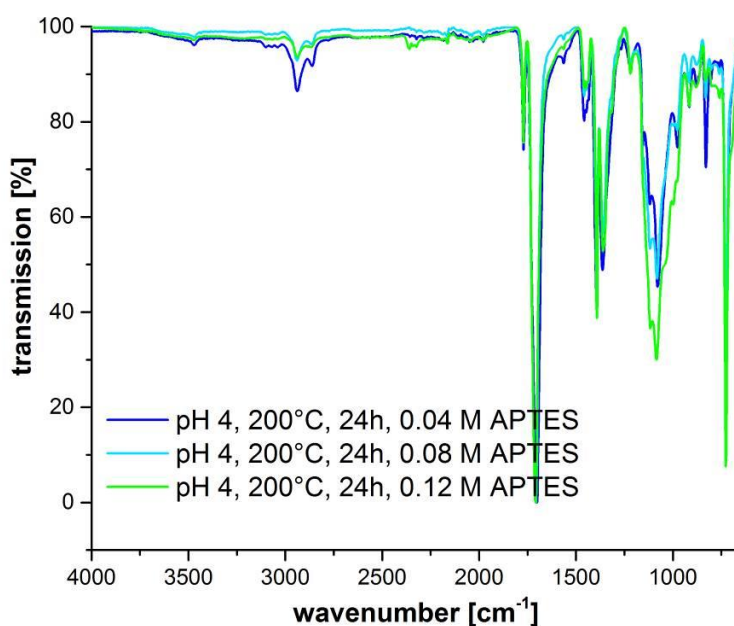


Figure 8: shows a superimposition of normalized FT-IR-ATR spectra of PI6/SiO₂-hybrids obtained from HDMA, PMA, and APTES(#7-9) at 200 °C and pH4 with different APTES concentrations Full conversion at all APTES concentrations ($\tilde{\nu}_{s,C=0}(\approx 1765\text{ cm}^{-1}$, $\tilde{\nu}_{as,C=0} \approx 1700\text{ cm}^{-1}$ and $\tilde{\nu}_{ar-H}$: 3101 and 3035 cm^{-1} ; $\tilde{\nu}_{alkyl-H}$: 2941, 2858 cm^{-1}). Siloxane vibration is also present ($\tilde{\nu}_{as}(\text{Si-O-Si}) \approx 1080\text{ cm}^{-1}$)

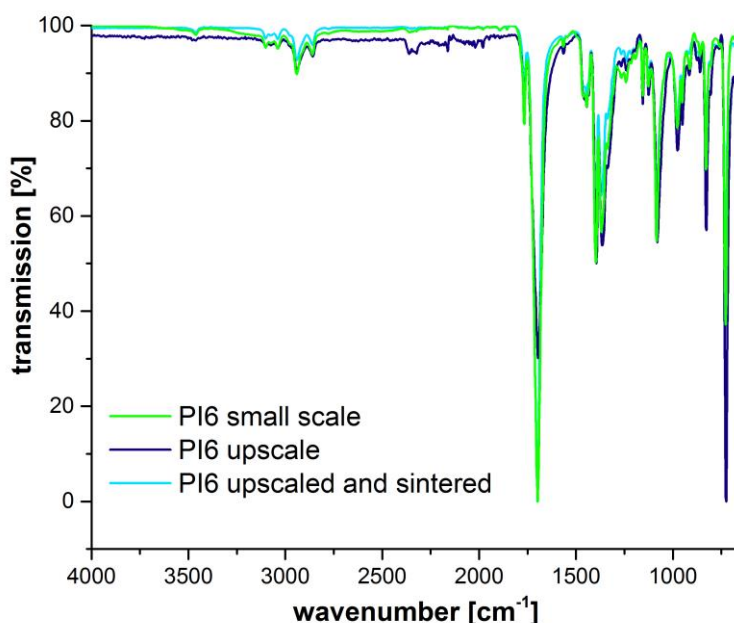


Figure 9: Superimposition of pure PI6 upscaled before and after sintering

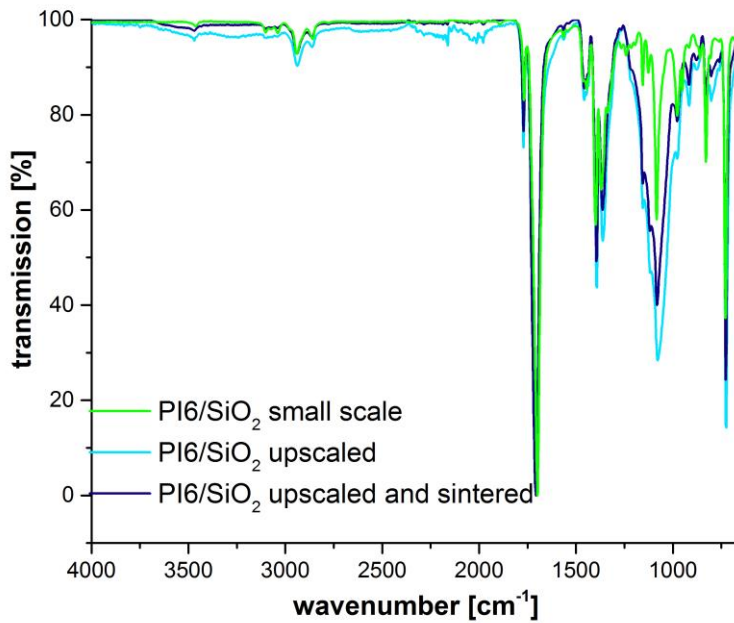


Figure 10: Superimposition of PI6/SiO₂ before and after sintering.

2.2 Powder X-ray diffraction (pXRD)

PXRD was collected using a PANalyticalX'Pert Pro multi-purpose diffractometer (MPD) in Bragg Brentano geometry operating with a Cu anode at 40 kV, 40 mA and an X-Celerator multichannel detector was used. Samples were ground and mounted as loose powders on silicon single crystal sample holders. The diffraction patterns were recorded between 5 and 60° (2θ) with 69.215 s/step and a step size of 0.0050134°, sample holders were rotated during the measurement with 4s/turn.

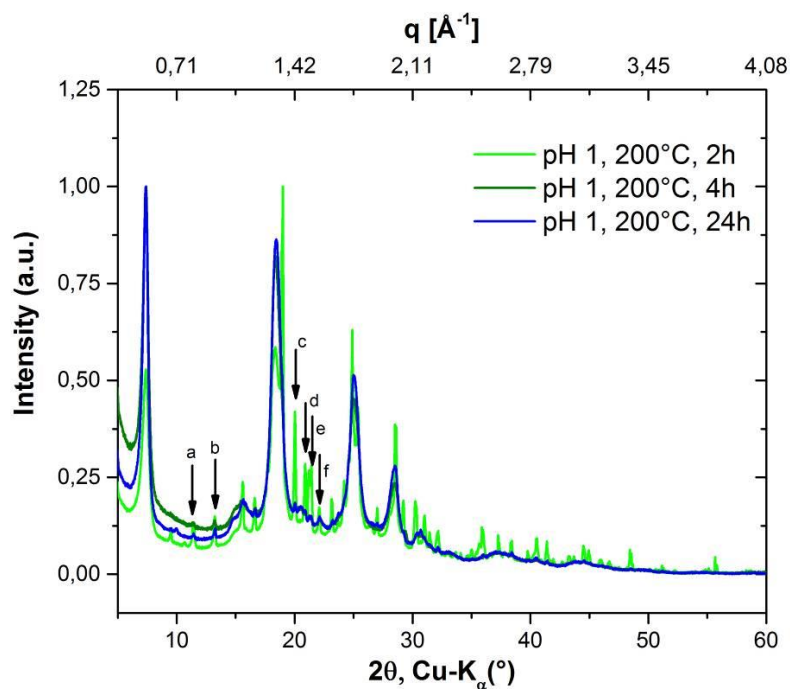


Figure 11: PXRD patterns of HT-PI obtained at different reaction times at 200 °C and pH 1. Peaks attributed to unreacted monomer salt and oligomers are present in the pattern of the sample obtained after 2 h and are denoted by (a-f). The PXRD pattern of products obtained after 4 and 24 h correspond to the typical HT-PI pattern.

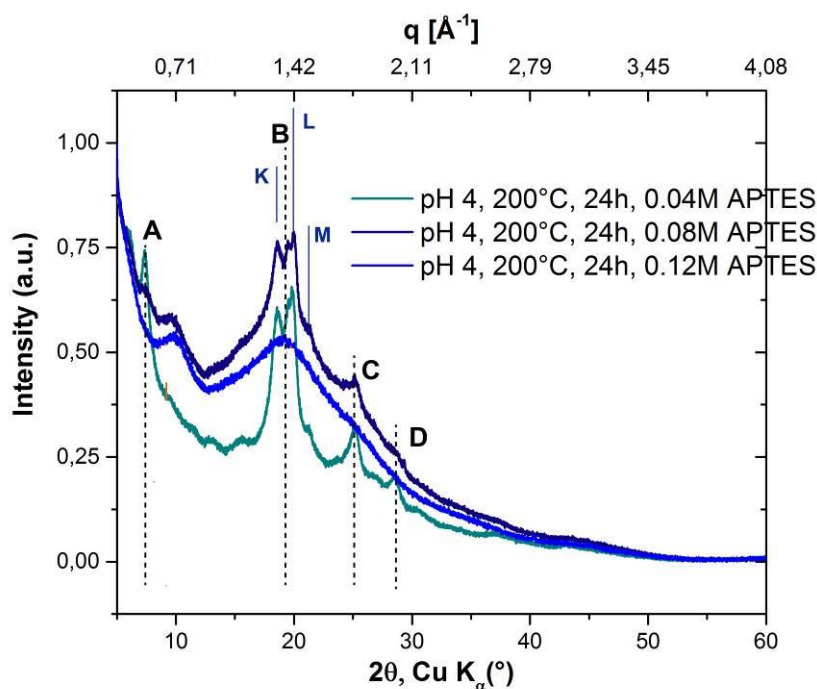
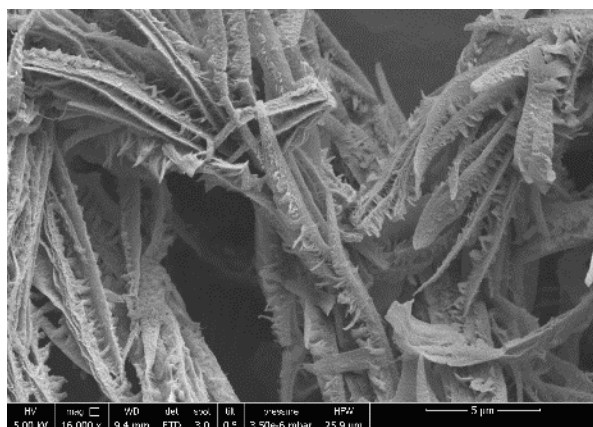


Figure 12 shows the PXRD patterns of PI6/SiO₂-Hybrids obtained from HDMA, PMA and APTES at 200 °C and pH 4 with different APTES amounts: Pattern shows all major reflections(A-D) (7.3°, 18.5°, 25.1° and 28.4°) in coexistence with new reflections. (K-M)(18.6°, 20.0° and 21.0°). Two amorphous halos are also centered around 9 and 19°.

2.3 Scanning electron microscopy (SEM)

Scanning electron microscopy was carried out with a *Quanta 200F FEI* microscope. Typically the samples were measured at 10 kV or 5 kV, with a working distance of 9 mm and spot size 2.0 or 3.0. Prior to imaging, samples were loaded on carbon coated stubs and coated by sputtering with an 8nm thick layer of Au/Pd 60/40 alloy with a *Quarum Q105T S* sample preparation system.

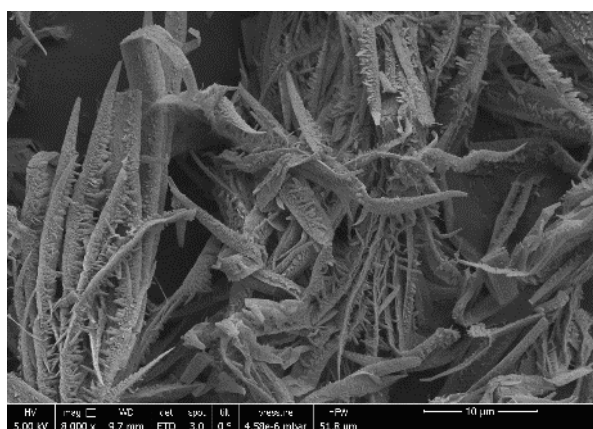
A



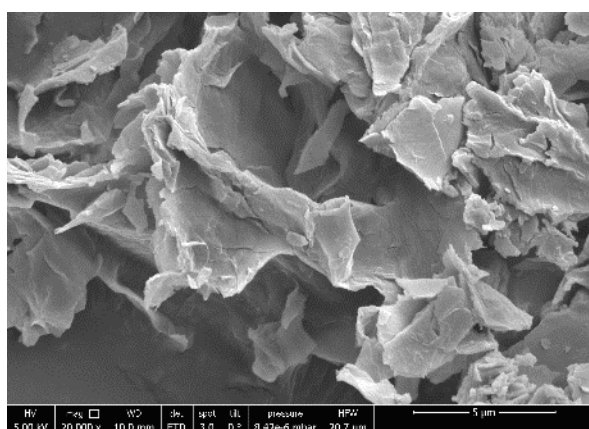
B



C



D



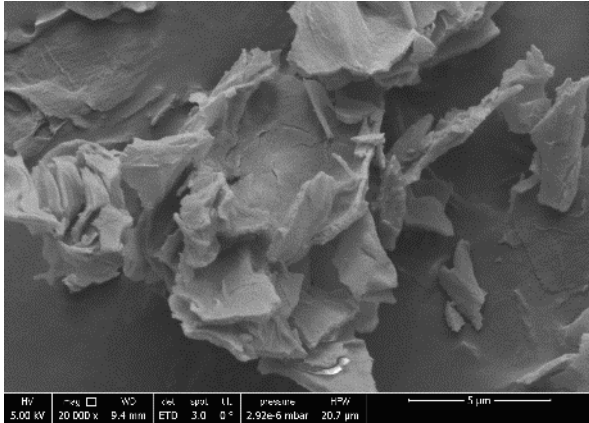
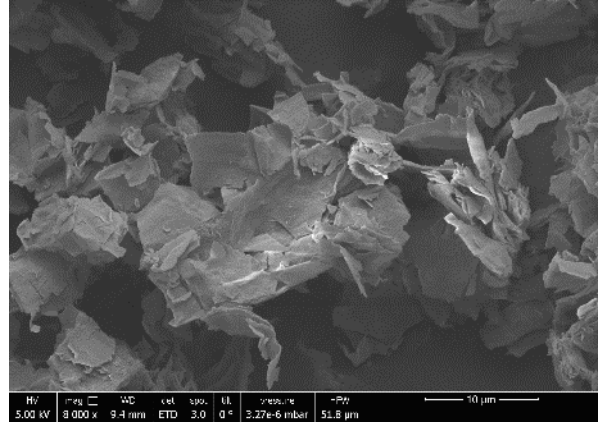
E**F**

Figure 13: shows SEM micrographs of PI6 synthesized at different pH (A-C) PI6 with ribbon morphology at pH 4 and 200°C after 2 h (A), 4 h (B) and 24 h (C), (D-F) PI6 with platelet-type morphology at pH 1 and 200°C after 2 h (D), 4 h (E) and 24 h (F).

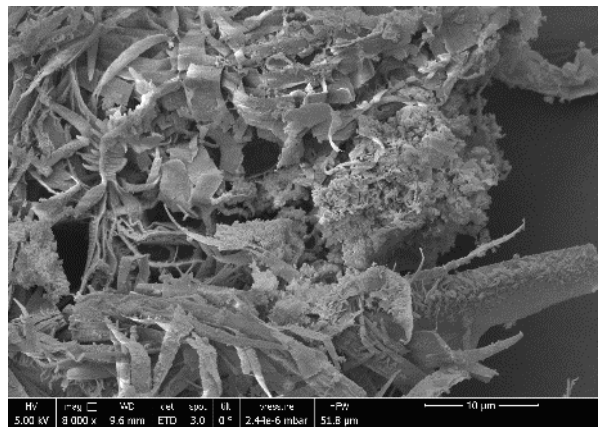
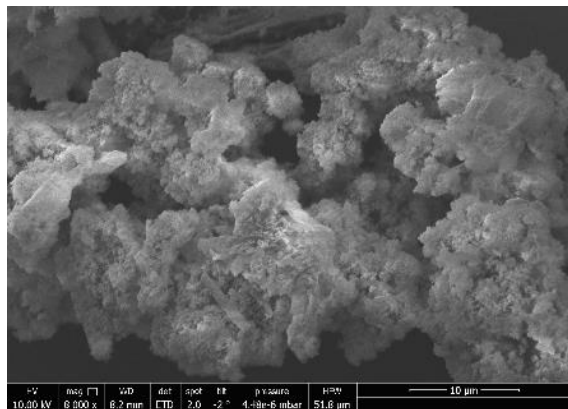
A**B****C**

Figure 14: SEM micrographs of PI6/SiO₂ hybrids obtained from HDMA, PMA and TEOS at different TEOS concentrations; 0.1M (A), 0.2 M (B) and 0.5 M(C) Ribbon morphology is retained at all 3 TEOS concentrations (see Figure 14). But the relative number of spherical nanoparticles increases with increasing TEOS amount.

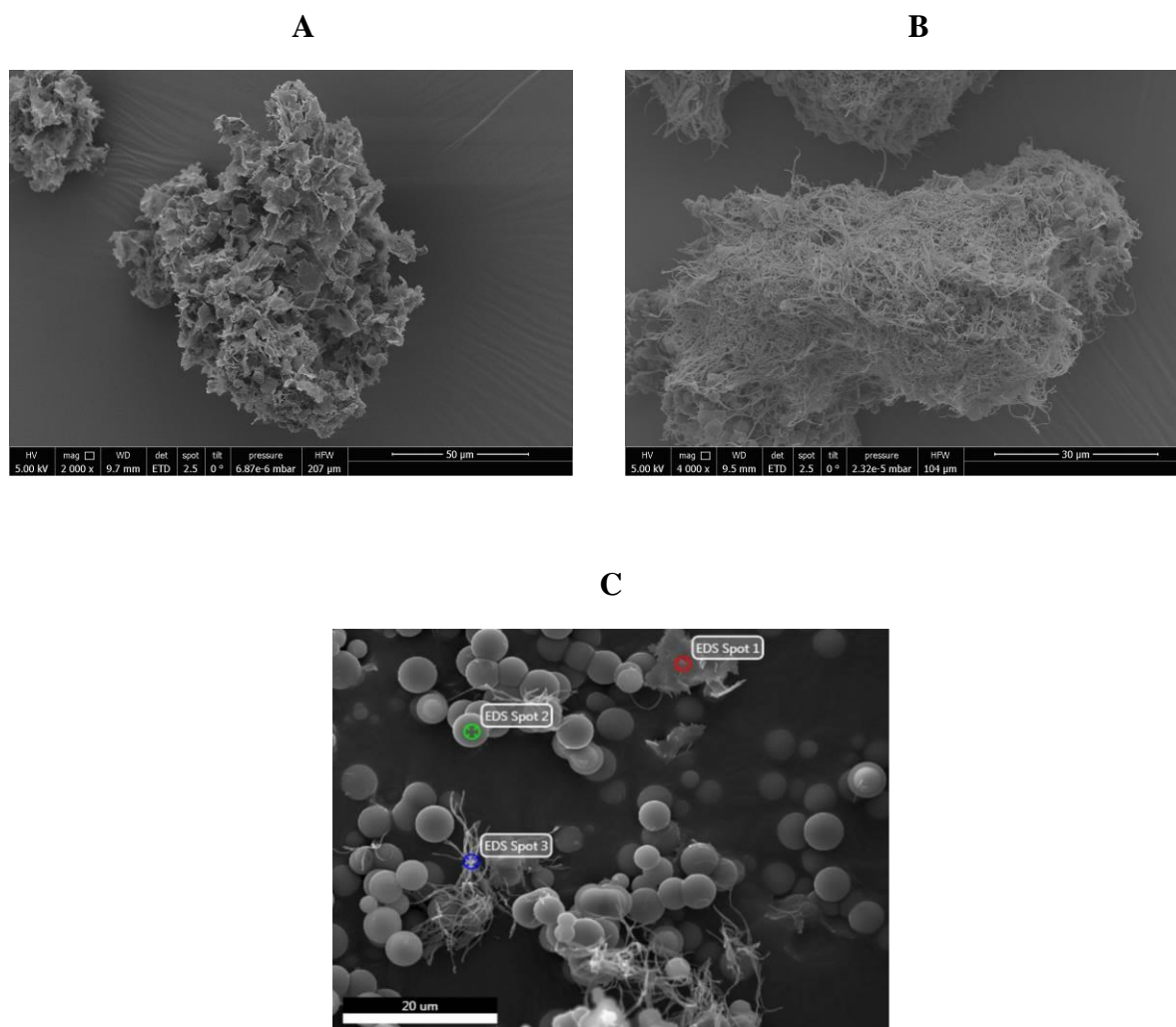


Figure 15: overview SEM micrographs of PI6/SiO₂–hybrids obtained from HDMA,PMA, TEOS and APTES with different APTES concentrations (#4-6). 0.6 mmol (A); 0.9 mmol (B) and 1.2 mmol (C) (see Figure 6)

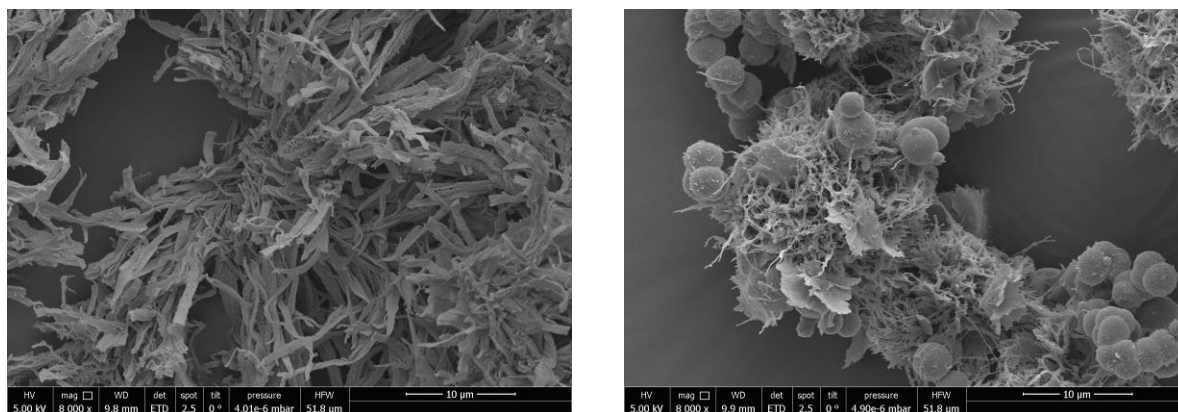


Figure 16: SEM micrographs of PI6/SiO₂- hybrids obtained from HDMA, PMA and 0.6 mmol APTES (left) and 0.9mmol APTES (right) With increasing n_{APTES} the amount of spherical particles relative to fibres increases.

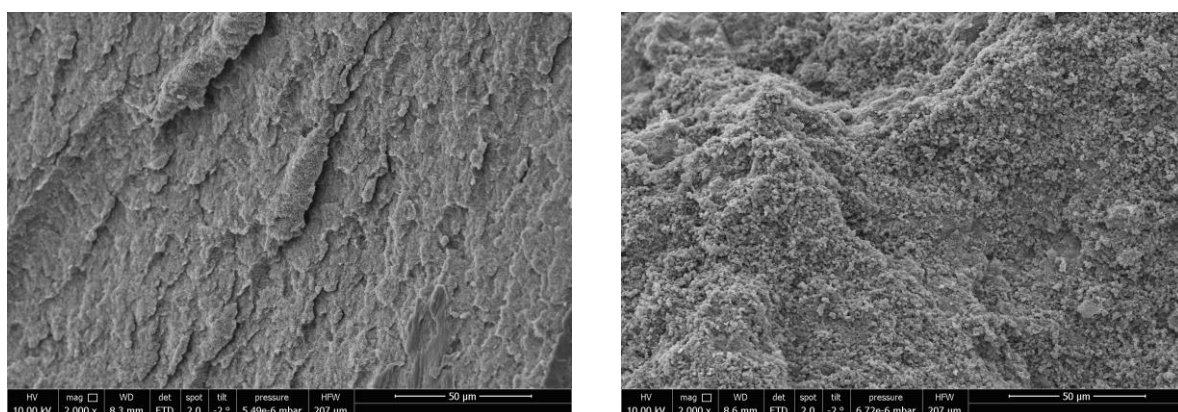


Figure 17: overview SEM micrographs of PI6 (left) and PI6/SiO₂ (right) after sintering

2.4 Energy-dispersive X-ray spectroscopy (EDAX)

Energy-dispersive X-ray spectroscopy was carried out with *Quanta 200F FEI* microscope and the Octane Elite Super X-ray detector. The samples were typically measured at 10kV. with a working distance of 10 mm and spot size 4.0. Prior to imaging, samples were loaded on carbon coated stubs and coated by sputtering with an 8nm thick layer of Au/Pd 60/40 alloy with a Quarum Q105T S sample preparation system (see SEM) Peaks labeled with Au and Pd come from the sputtering layer and the C peak is part arising from the carbon stubs.

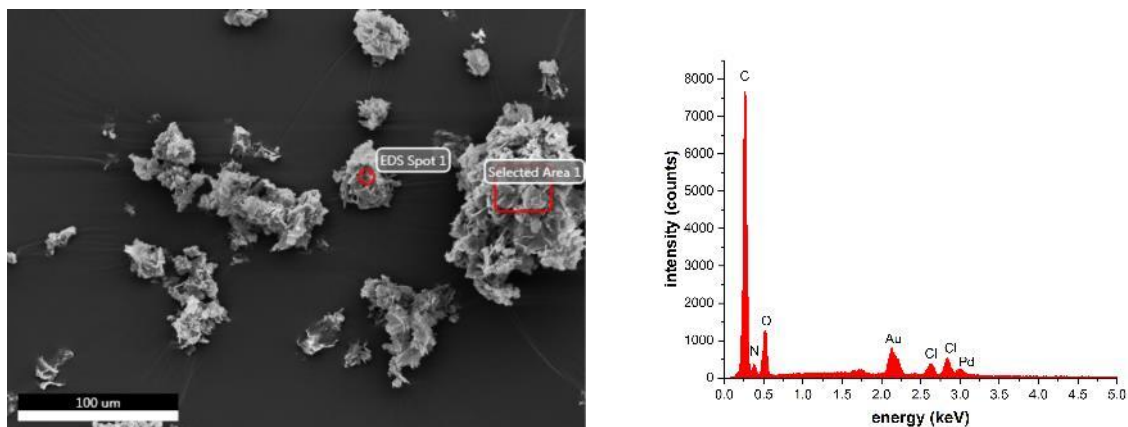


Figure 18: SEM micrograph of PI6 synthesized at pH 1 with corresponding EDAX spectrum of area 1. Polyimide formed at pH 1 contains Cl.

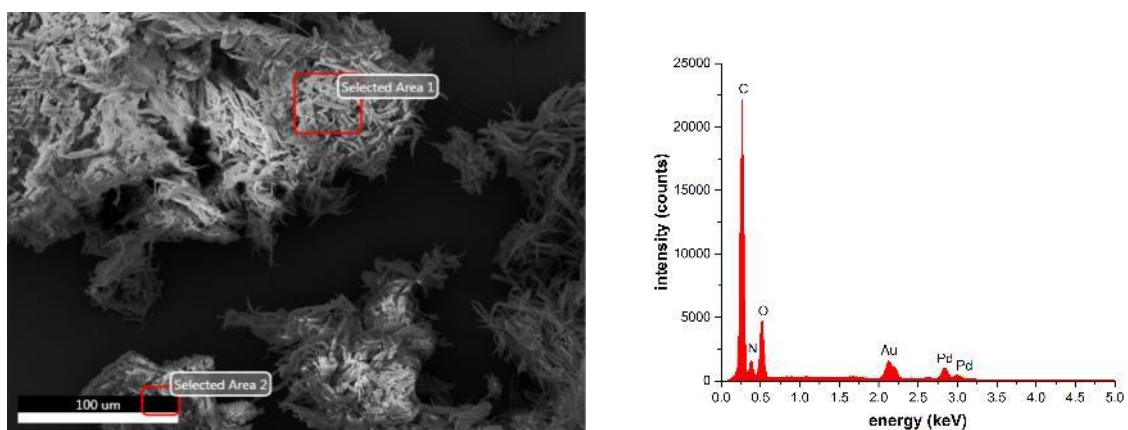


Figure 19: SEM micrograph of PI6 synthesized at pH 4 with corresponding EDAX-spectrum of area 1. Polyimide formed at pH 4 contains exclusively C, N and O.

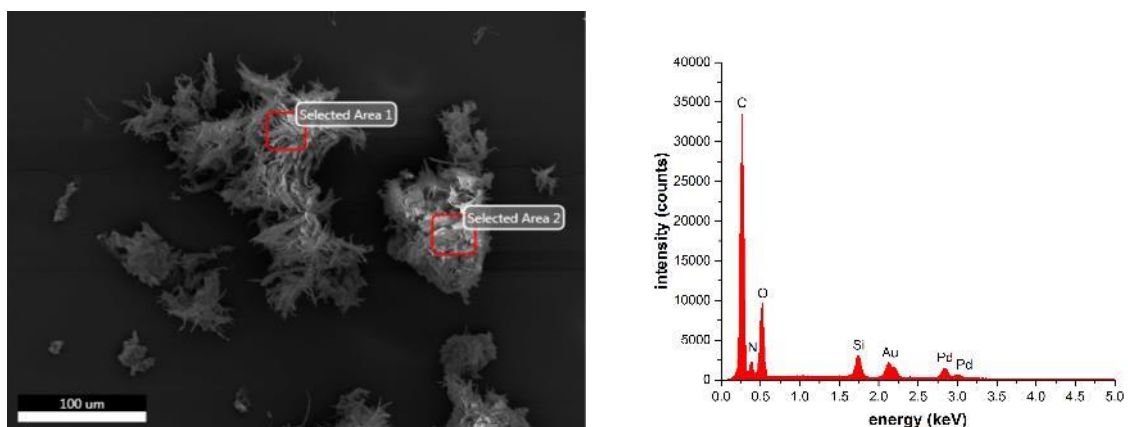


Figure 20: SEM micrograph of PI6/SiO₂ hybrid prepared using 1.5 mmol TEOS with corresponding EDAX-spectrum of area 1. Hybrid contains besides C, N and O also Si

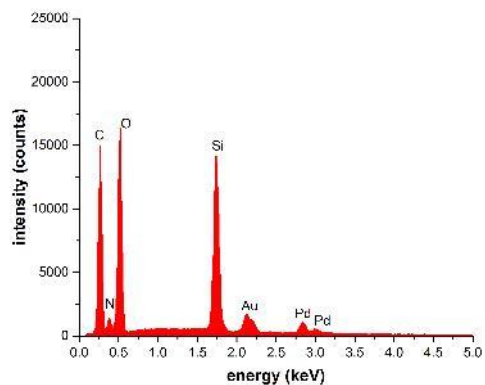
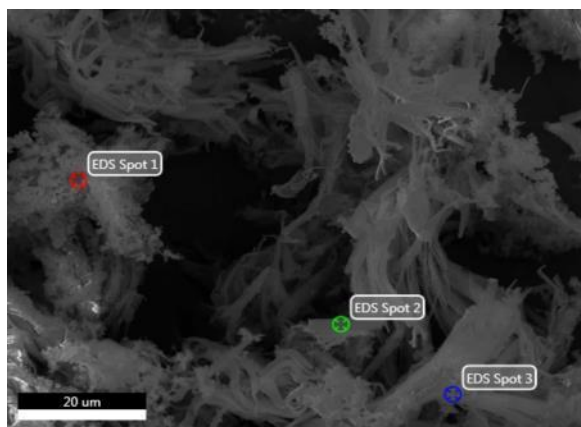


Figure 21: SEM micrograph of PI6/SiO₂ hybrid obtained from HDMA, PMA and TEOS prepared using 3.0 mmol TEOS with corresponding EDAX spectrum of spot 1: Hybrid contains besides C, N and O also Si

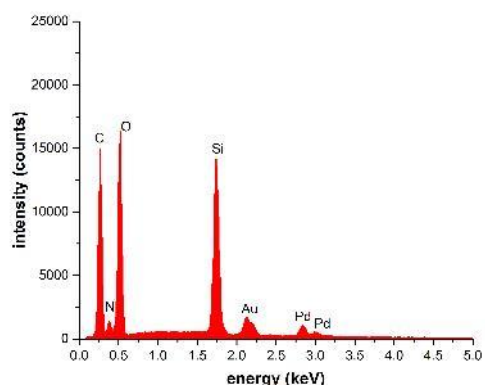
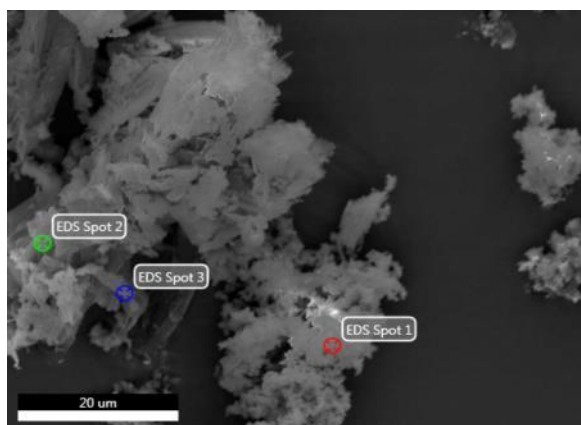


Figure 22: SEM micrograph of PI6/SiO₂ hybrid obtained from HDMA, PMA and TEOS prepared using 7.5 mmol TEOS with corresponding EDAX spectrum of spot 1. Hybrid contains besides C, N and O also Si

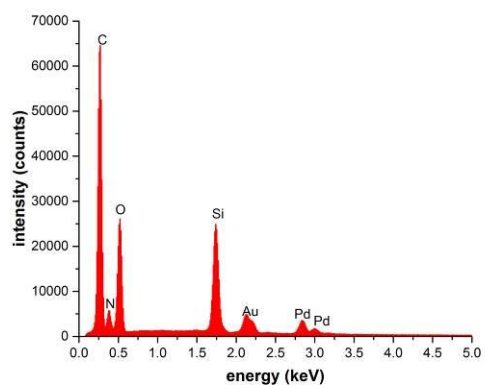
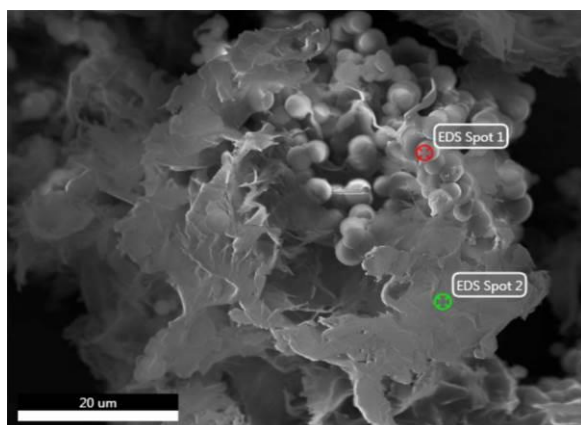


Figure 23: SEM micrograph of PI6/SiO₂ hybrid obtained from HDMA, PMA, APTES and TEOS prepared using 0.6 mmol APTES with corresponding EDAX spectrum of spot 2: Hybrid contains besides C, N and O also Si

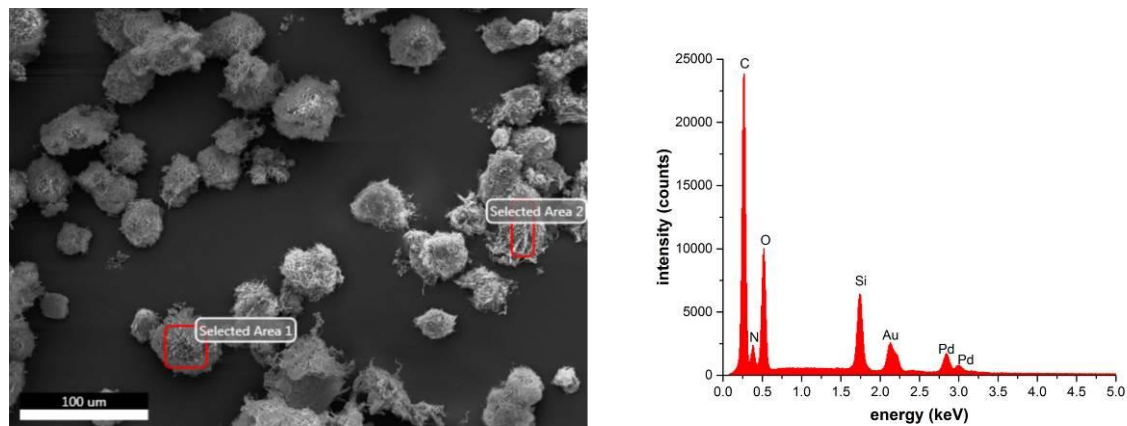


Figure 24: SEM micrograph of PI6/SiO₂ hybrid obtained from HDMA, PMA, APTES and TEOS prepared using 0.9 mmol APTES with corresponding EDAX spectrum of area 1: Hybrid contains besides C, N and O also Si

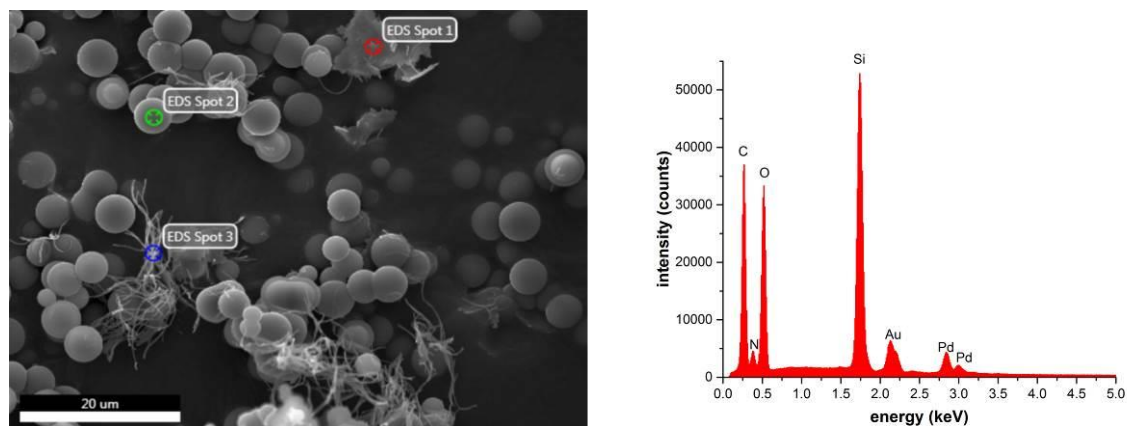


Figure 25: SEM micrograph of PI6/SiO₂ hybrid obtained from HDMA, PMA, APTES and TEOS prepared using 1.2 mmol APTES with corresponding EDAX spectrum of spot 2: The spheres contain a relatively high amount of Si.

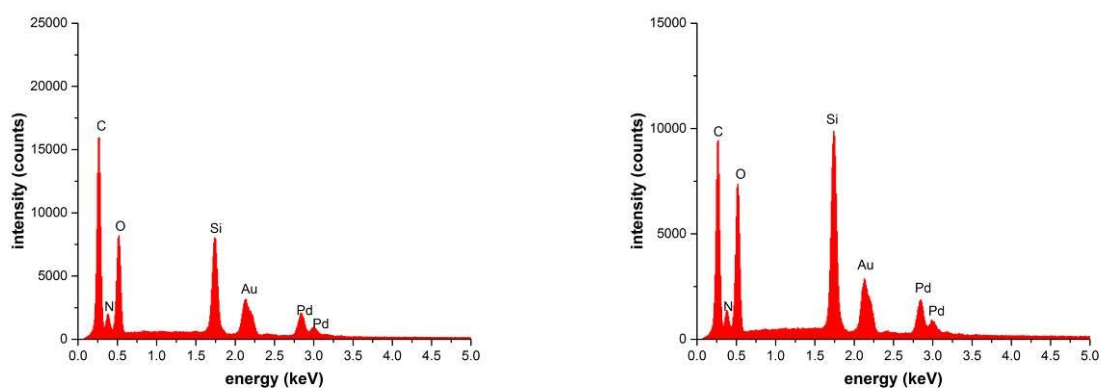
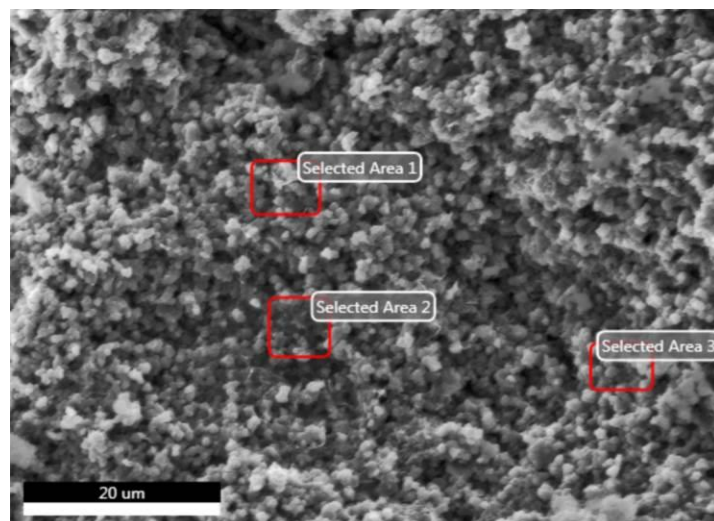


Figure 26: SEM micrograph and corresponding EDAX spectra of upscaled PI6/SiO₂ after sintering of area 2 (left) and area 3 (right)

2.5 Cross Polarization Magic Angle Spinning Nuclear Magnetic Resonance Spectroscopy (CP-MAS-NMR)

¹³C, ¹⁵N and ²⁹Si solid state NMR spectra were recorded on a Bruker AVANLE 300 (¹³C at 75.4 MHz, ¹⁵N at 30.38 MHz and ²⁹Si at 59.57 MHz equipped with a 4 mm broadband MAS probe head. Spectra were recorded with ramped CP MAS experiments (cross polarization and magic angle spinning). The sample holders were spun at 4kHz for ²⁹Si and ¹⁵N and 10 kHz for ¹³C.

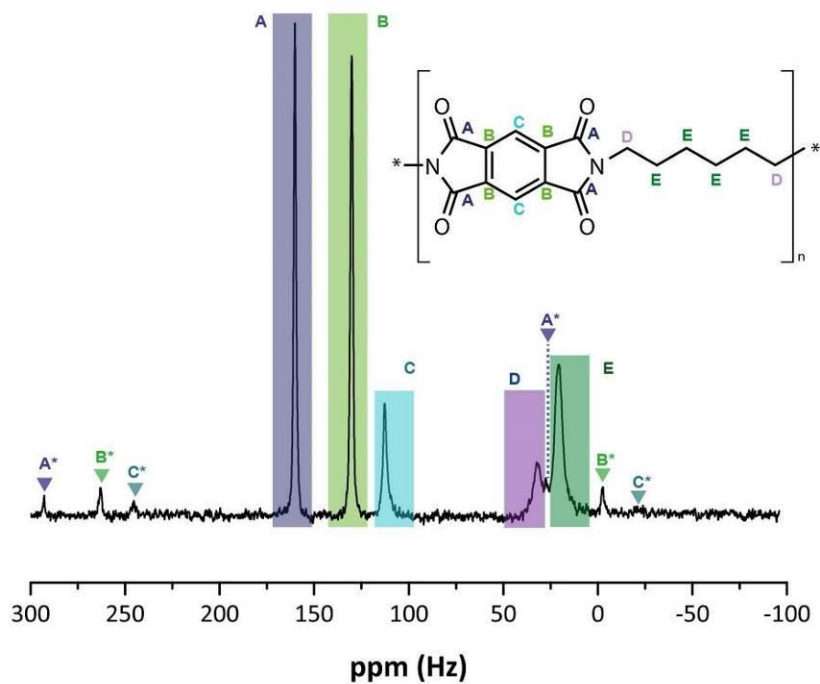


Figure 27: ^{13}C - NMR of pure PI6 scale up. Note that the signals attributed to A, B and C give rise to the spinning sidebands labelled as (A*, B*, and C*)

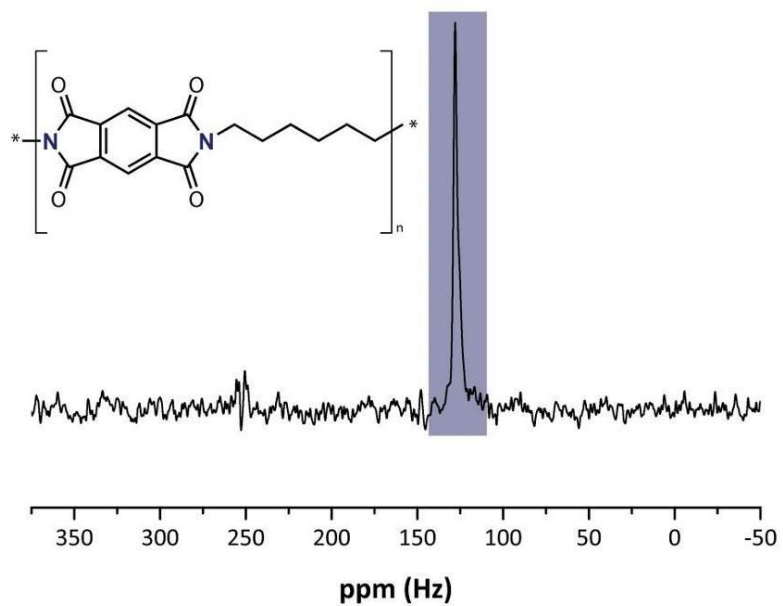


Figure 28: ^{15}N - NMR of pure PI6 scale up

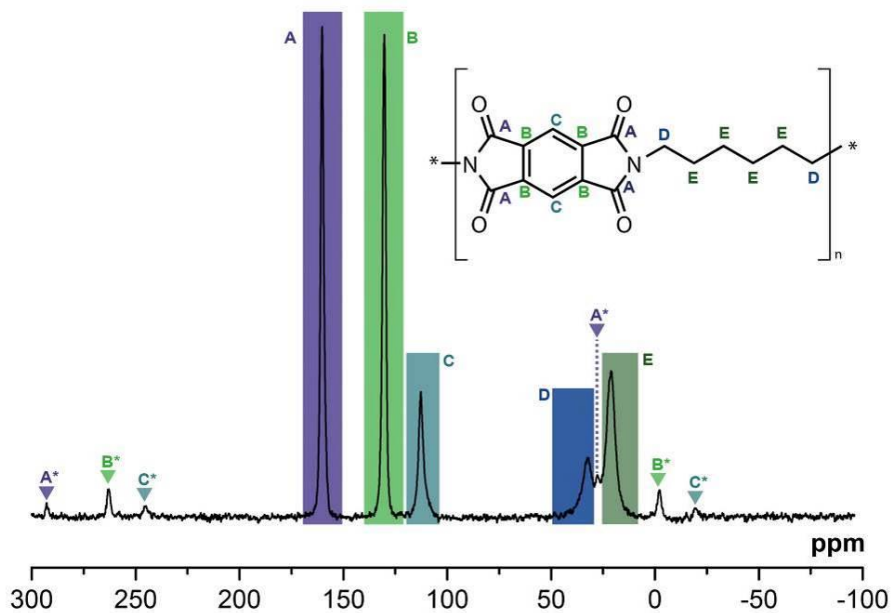


Figure 29: ^{13}C - NMR of pure PI6 scale up after sintering. Note that the signals attributed to A, B and C give rise to the spinning sidebands labelled as (A*, B*, and C*)

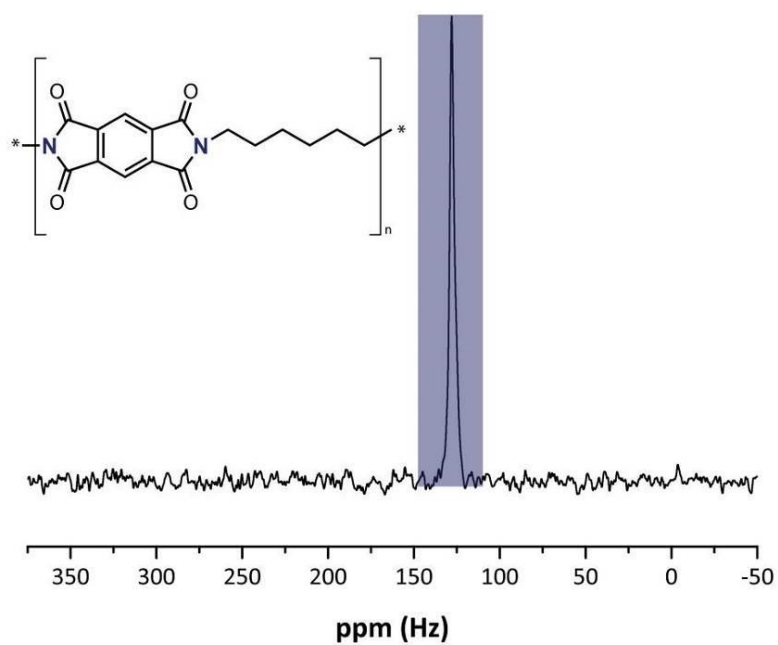


Figure 30: ^{15}N - NMR of pure PI6 scale up after sintering

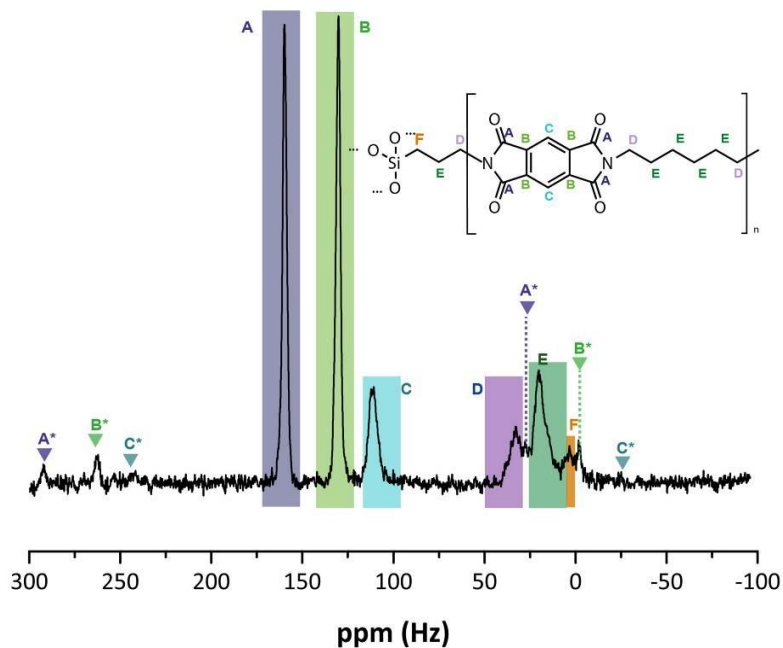


Figure 31: ^{13}C - NMR of PI6/SiO₂ scale up. Note that the signals attributed to A, B and C give rise to the spinning sidebands labelled as (A*, B*, and C*)

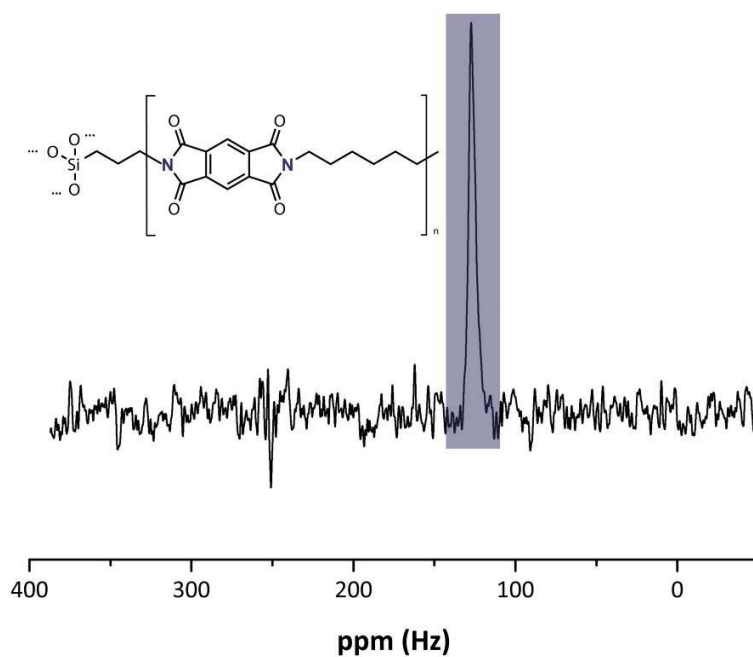


Figure 32: ^{15}N - NMR of PI6/SiO₂ scale up.

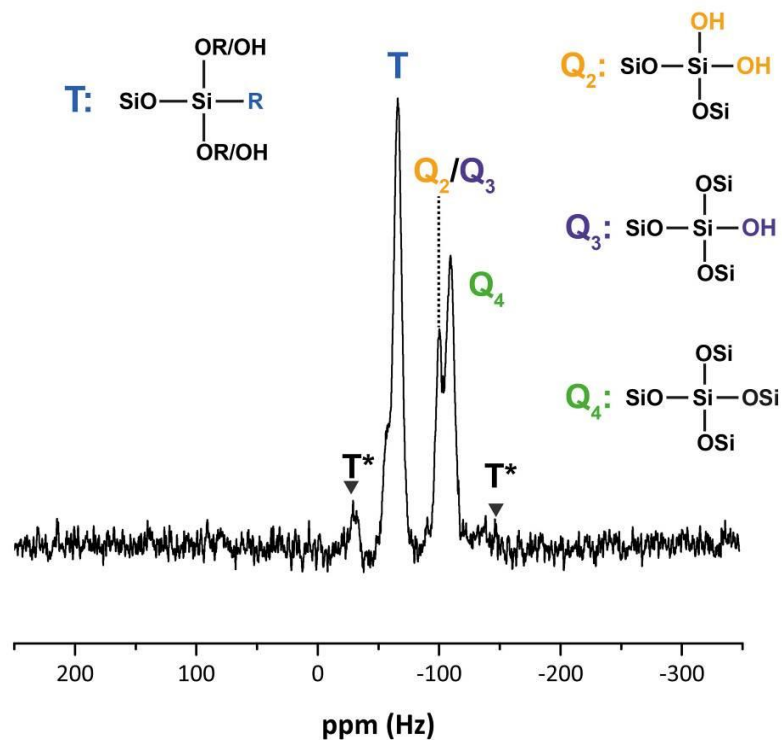


Figure 33: ^{29}Si -NMR of PI6/SiO₂ scale up. Note that the signals attributed to T give rise to the spinning sidebands labelled as (T*).

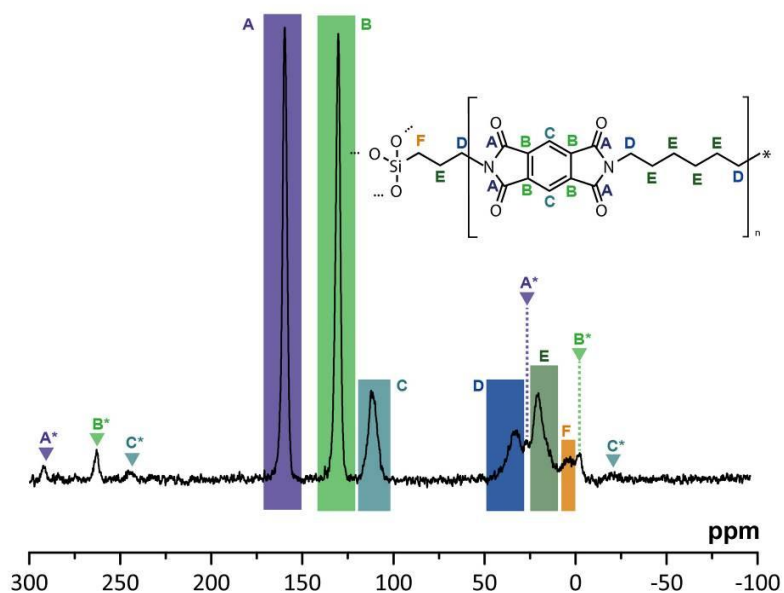


Figure 34: ^{13}C - NMR of PI6/SiO₂ scale up after sintering. Note that the signals attributed to A, B and C give rise to the spinning sidebands labelled as (A*, B*, and C*)

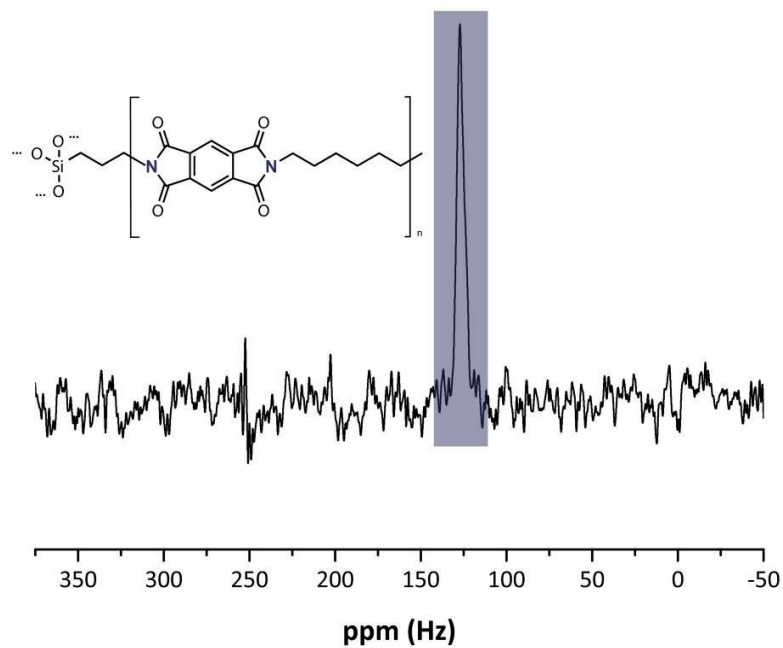


Figure 35: ^{15}N - NMR of PI6/SiO₂ scale up after sintering

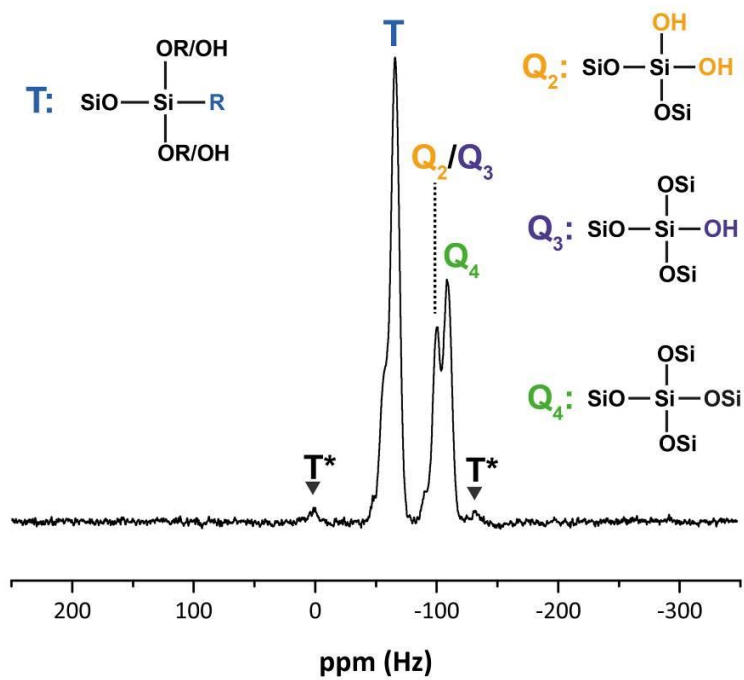


Figure 36: ^{29}Si - NMR of PI6/SiO₂ scale up after sintering. Note that the signals attributed to T give rise to the spinning sidebands labelled as (T*).

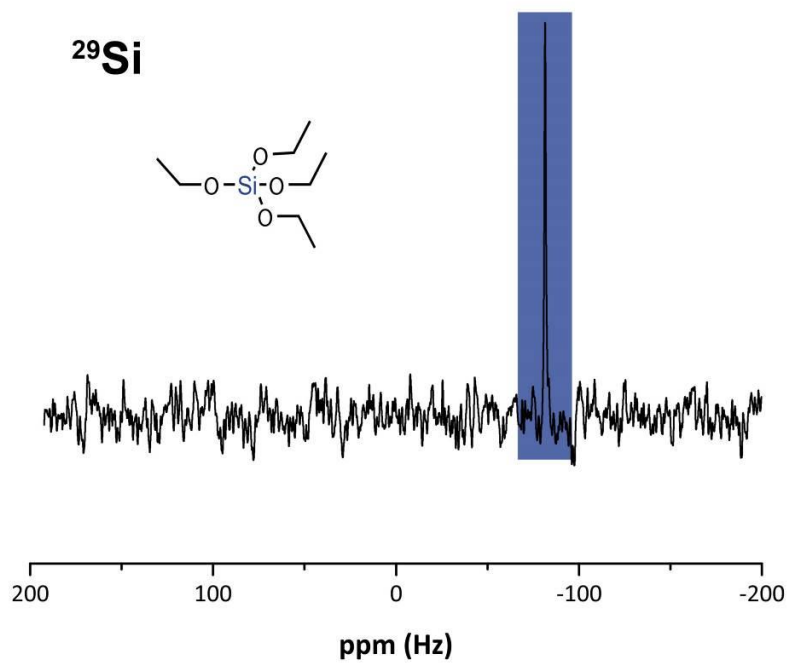


Figure 37: ²⁹Si NMR of TEOS

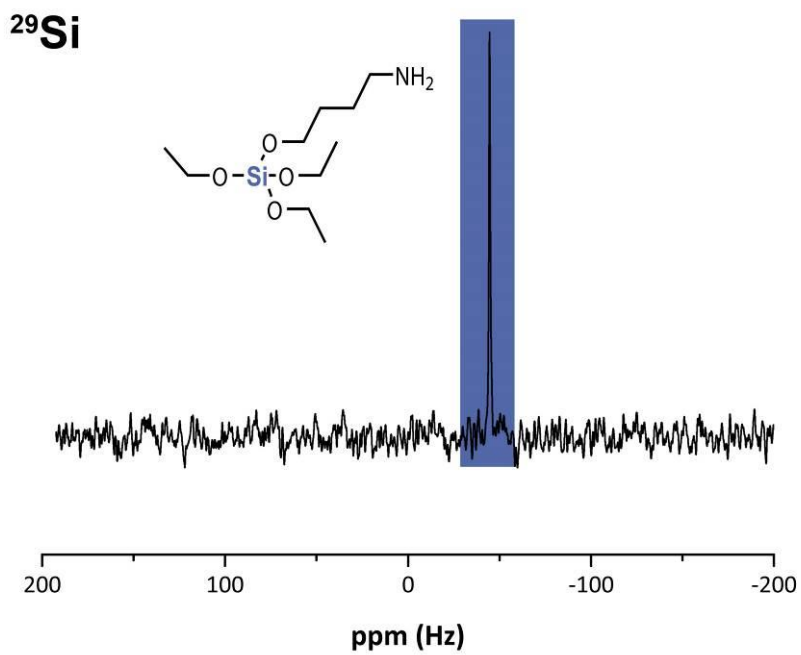


Figure 38: ²⁹Si NMR of APTES